DOI: 10.15669/pnst.8.104

Progress in Nuclear Science and Technology
Volume 8 (2025) pp. 104-109

ARTICLE

A Safety Enhanced Core Concept for Metal-Fuel Sodium-Cooled Fast Reactors

Sho FUCHITA [1*], Koji FUJIMURA [1], Kazuhiro FUJIMATA [1], Tomoki MISHIMA [1],
Hirotaka NAKAHARA [1], Satoshi TAKEDA [2] and Hirokazu OHTA [3]

[1] *Hitachi-GE Nuclear Energy, Ltd., 1-1 Saiwai-cho, 3-chome, Hitachi-shi, Ibaraki-ken, 317-0073, Japan*
[2] *Osaka University, 2-1 Yamadaoka, Suita-shi, Osaka, Japan*
[3] *Central Research Institute of Electric Power Industry, 2-6-1 Nagasaka, Yokosuka-shi, Kanagawa-ken, 240-0196, Japan*

A safety enhanced metal fuel core has been developed that prevents fuel pin failure and coolant boiling during unprotected loss of flow (ULOF), unprotected transient over power (UTOP) and unprotected loss of heat sink (ULOHS) without relying on radial expansion reactivity. Specifically, we have enhanced inherent reactivity feedback and added passive shutdown devices without significantly changing core specifications and economic performance. The neutron flux distortion during UTOP situation with the control rod withdrawal and the neutron flux changes around the gas expansion module (GEM) during ULOF transient are also confirmed by improved quasi-static approximations. Both local neutron flux changes lead to a power increase, but even taking them into account, the inherent reactivity feedback and reactivity brought by passive devices in the safety enhanced metal fuel core are sufficient to prevent core damage under ULOF, UTOP and ULOHS conditions.

KEYWORDS: sodium-cooled fast reactor, metal fuel core, anticipated transient without scram, gas expansion module, self-actuated shutdown system, reactor vessel auxiliary cooling system

I. Introduction

A feature of the metal-fuel core from the point of view of core safety is the good chemical coexistence of the metal fuel and sodium, and the gap conductance can be significantly reduced by sodium bonding in the fuel cladding. In addition, the thermal conductivity of the metal fuel is higher than that of the MOX fuel. These characteristics promote heat transfer from the fuel alloy to the coolant and reduce the maximum fuel alloy temperature, thereby compensating for the lower melting point of metallic fuel. This feature also has the benefit of reducing the reactivity difference between the zero power state and the full power state, which makes it easier to transition from the full power state to the hot standby state, even during Anticipated Transients Without Scram (ATWS), due to inherent reactive feedback, such as core radial expansion reactivity.[1)]

However, the core radial expansion behavior is a complex phenomenon involving the core restraint conditions, structural material properties and temperature distributions, and the development of high-precision evaluation methods is still ongoing. Therefore, we are developing a safety enhanced metal fuel core that can prevent pin failure and coolant boiling without radial expansion reactivity for ATWS including Unprotected Loss of Flow (ULOF), Unprotected Transient Over Power (UTOP), and Unprotected Loss of Heat Sink (ULOHS).

II. Concepts

The main specifications of the safety enhanced core were based on those of a small metal fuel fast reactor core as the reference core.[2,3)] The reference core had passive safety systems, such as Gas Expansion Module (GEM), rod stop and Reactor Vessel Auxiliary Cooling System (RVACS).

In this study, we added safety enhancement measures based on the reference core concepts to compensate for the assumption that no radial expansion reactivity is expected. Specifically, B4C absorbers were installed behind the GEMs to improve their effectiveness, and a Self-Actuated Shutdown System (SASS)[4)] was installed. In addition, the core fuel assemblies had larger diameter pins compared to the reference core. This results in a reduction in coolant volume and an increase in fuel volume. As a result, coolant void reactivity decreases. In addition, the decrease in Pu enrichment due to the increase in the fuel volume leads to an increase in the fertile fraction in the center of the core, which improves the internal conversion ratio and reduces the burnup reactivity. Furthermore, the core had an Axial Heterogeneous Core (AHC), which is expected to improve fuel integrity by suppressing the Maximum Linear Heat Generation Rate (MLHGR) and to make the flow distribution more efficient by suppressing the change in the assembly power due to burnup.

The aim of the safety enhanced core concept is to prevent coolant boiling and fuel damage through passive safety measures for ULOF, UTOP and ULOHS situations.

Specifically, for ULOF, reactor shutdown by SASS is expected and coolant boiling is avoided by GEM and inherent reactivity feedback until SASS is activated. Similarly, for UTOP, reactor shutdown by SASS is expected and fuel

*Corresponding author, E-mail: sho.fuchita.bj@hitachi.com

damage is avoided by rod stop and inherent reactivity feedback until SASS is activated. For ULOHS, coolant boiling is avoided by grid plate expansion reactivity and cooling by RVACS.

Figure 1 shows the safety enhanced core configuration. 6 Primary Control Rods (PCRs) with rod stop, 3 Backup Control Rods (BCRs) with SASS and 6 B4C absorbers with 6 GEMs behind them were installed. These measures can be applied without occupying additional core space, as they are retrofitted to the control system or replace existing reflectors.

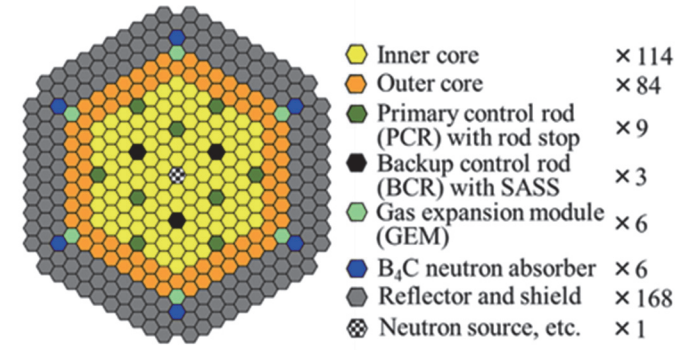

(a) Horizontal section

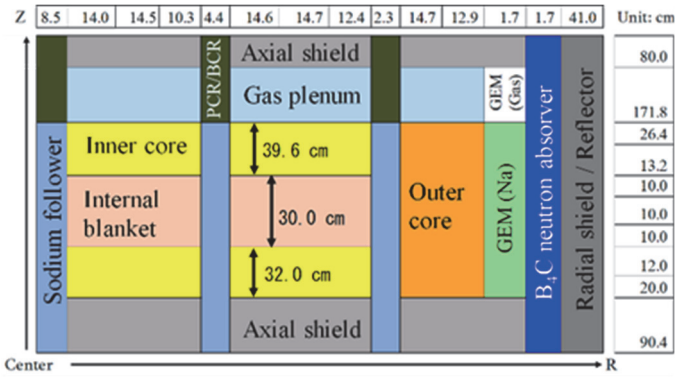

(b) Vertical section

Fig. 1 Core configuration of the safety enhanced core

III. Design Criteria and Methods

For evaluation of the safety enhanced core, we analyzed core neutronic characteristics and fuel irradiation behavior during normal operation and transient behavior during ULOF, UTOP and ULOHS.

The design criteria are shown in **Table 1**. The design criteria were set based on previous studies[2,3,5-7] of metallic fuel cores. Specifically, the sodium void reactivity was set at 8$ or less to avoid prompt criticality due to molten fuel movement during the ULOF initiation phase,[5] the MLHGR was set at 500 W/cm or less to avoid fuel melt during normal operation,[5] and the Pu enrichment was set at 25 wt.% or less to be within the range of experimental data for preventing liquid phase formation due to fuel clad chemical interaction during normal operation.[6] In addition, the average discharge burnup and the operating cycle period target were set based on previous studies.[5] Cumulative creep damage fraction (CDF) limit of fuel cladding was set to 0.5 at the time of fuel removal to prevent pin failure during normal operation. The power to flow ratio limit during ULOF was set to prevent sodium boiling based on core inlet and outlet temperatures. The SASS operating temperature was set at 680℃ , based on the temperature required for delatch, referring to previous studies.[7]

Table 1 Design criteria in neutronic, fuel irradiation behavior and ATWS analysis.

Item	Target
Thermal power	= 840 MWt [2,3]
Primary sodium inlet / outlet temperature	= 360℃ / 499℃ [2,3]
Primary sodium flow rate	= 4675 kg/s [2,3]
Sodium void reactivity	≤ 8 $[5]
Maximum linear heat generation rate	≤ 500 W/cm[5]
Pu enrichment (Pu/HM)	≤ 25 wt.%[6]
Average discharge burnup excluding blanket	≒ 100 GWd/t[5]
Operation cycle period	≥ 550 EFPD[5]
Cumulative creep damage fraction in normal operation / UTOP situation	≤ 0.5 / ≤ 1.0
Maximum sodium temperature / Power to flow ratio limit in ATWS situation	≤ 960℃ / ≤ 2.5
SASS actuation temperature	= 680℃[7]
PCR withdrawal reactivity limit by rod stop / reactivity insertion rate in UTOP situation	= 20 cents / 3 cents/s

Figure 2 shows burnup calculation flowchart. The calculations were performed with the core configuration and Effective Full Power Day (EFPD) set to meet the design conditions of Pu enrichment and average discharge burnup. Burnup characteristics and reactivity coefficients were calculated by MARBLE[8] based on diffusion theory using a two-dimensional R-Z model with a seventy-group cross section library UFLIB.J40 for fast reactors based on JENDL-4.0.[9] However, the neutron leakage effect dominates the GEM reactivity, and the evaluation by diffusion theory is not sufficient. Therefore, the reactivity of GEMs was evaluated

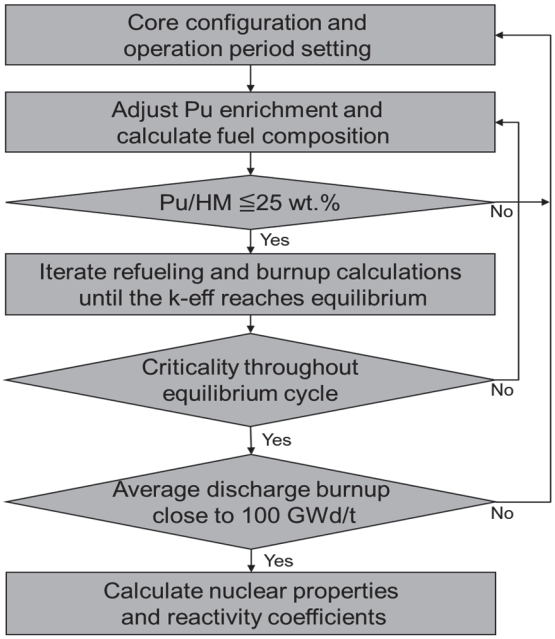

Fig. 2 Burnup calculation flowchart

by the SN neutron transport calculation code MINISTRI[10] with a three-dimensional TRI-Z model.

The fuel irradiation behavior and CDF of the peak power fuel cladding were analyzed by the metal fuel irradiation behavior analysis code ALFUS.[11] In the fuel behavior analysis, the flow rate around the fuel pin was set to reach the maximum fuel temperature of 650◦C under normal operation as a conservative assumption. In addition, to estimate the relative power leading to cladding failure during UTOP, the history of CDF for peak power fuel cladding was calculated assuming continuous reactivity insertion at 3 cents/s.

The transient behavior during ATWS was calculated by FOSTER[12] based on the point kinetics equation. This analysis considered the reactivity change due to expansion caused by temperature changes in the fuel, coolant, cladding, and wrapper as well as doppler reactivity. In addition, the ULOF analysis considered GEM reactivity, the UTOP analysis considered reactivity with a primary control rod withdrawal and the ULOHS analysis considered the grid plate expansion reactivity caused by the increase in core inlet temperature. In the ULOF and UTOP analyses, the core inlet temperature was set constant at 360°C, but in the ULOHS analysis, the inlet temperature was calculated value considering coolant circulation and RVACS cooling. The coolant flow rate during the ULOF analysis was referred to the CFD calculation considering the electromagnetic pump shutdown.[13] Furthermore, the calculations of improved quasi-static approximation by KICOM[14] were also performed in the ULOF and UTOP analysis to confirm the influence of the GEM activation and the control rod withdrawal on the neutron flux distribution change. To ensure conservative conditions, the ULOF analysis considered GEMs failures, the UTOP analysis considered the conservative SASS activation time, and the heat removal by the intermediate heat exchanger was set to zero immediately at the start of the ULOHS analysis.

IV. Results and Discussion

1. Core Neutronic Analysis

Table 2 shows analysis results of the core neutronic characteristics. All design criteria set in the previous chapter were achieved by adjusting the operation period and Pu enrichment. The MLHGR of the safety enhanced core is less than 300 W/cm, which is reduced compared to the reference core value, due to the AHC configuration. These results are based on a two-dimensional R-Z model and do not consider three-dimensional effects such as fuel exchange patterns, but even if these are considered, the MLHGR is not expected to exceed the 500 W/cm limit. No burnup reactivity limit was set in this study, but the value of the safety enhanced core was lower than that of the reference core due to larger diameter fuel pin, which contributes to the reduction of the reactivity insertion potential when the control rods withdrawal. The reactivity of the 6 GEMs was approximately -0.6 $, which was increased by about 1.4 times due to the installation of B4C neutron absorbers behind GEMs. This is because when the GEM is activated, the B4C neutron absorber captures the leaked neutrons and prevents them from scattering towards the core region. Overall, safety has been improved while maintaining the same economic efficiency compared to the reference core.

Table 2 Analysis results of core neutronic characteristics

Item	Value	Reference core value[15]
Core configuration	Axial heterogeneous	Radial heterogeneous
Fuel pin outer diameter	8.907 mm	7.44 mm
Pu enrichment (Pu/HM)	18.4 / 22.2 wt.% (Inner / Outer core)	23.7 wt.%
Burnup period	580 EFPD × 4 batches	598 EFPD × 3 batches
Maximum linear heat generation rate	282 W/cm	357 W/cm
Average discharge burnup	106 / 95 GWd/t (Inner / Outer core)	106.3 GWd/t
Burnup reactivity	3.7 $	5.1 $
Sodium void reactivity	5.8 $	6.0 $
GEM reactivity	-0.62 $	-0.42 $

2. Fuel Behavior Analysis

Figure 3 shows fuel behavior analysis results. The history of the maximum cladding temperature does not decrease much for the inner core fuel, but for the outer core fuel temperature decreases by about 100°C between the initial loading and the removal phase. This is because the outer core fuel does not have an internal blanket, so there is no increase in power in the blanket region due to burnup. As a result, as shown in **Fig. 4**, the CDF value of the inner core fuel, which remains in a high temperature state, is higher than that of the outer core fuel. However, the highest CDF value is 0.04,

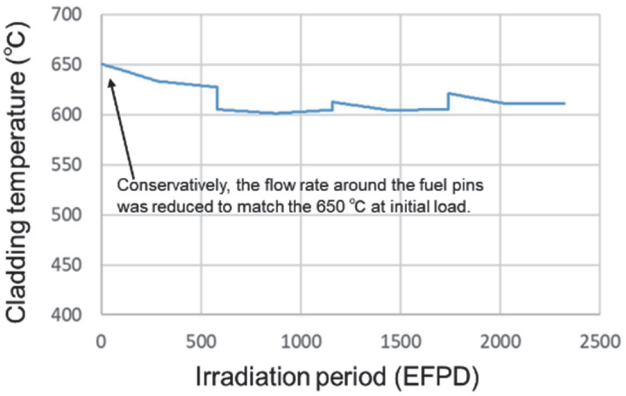

(a) Inner core fuel

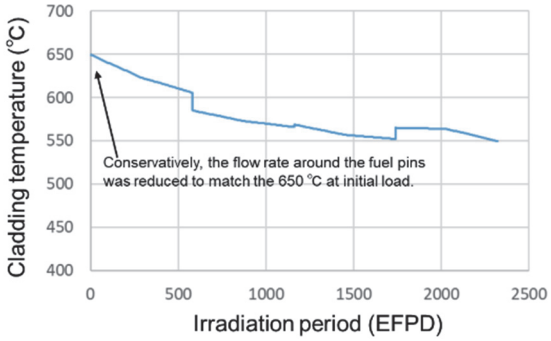

(b) Outer core fuel

Fig. 3 Maximum cladding temperature history for peak power pin

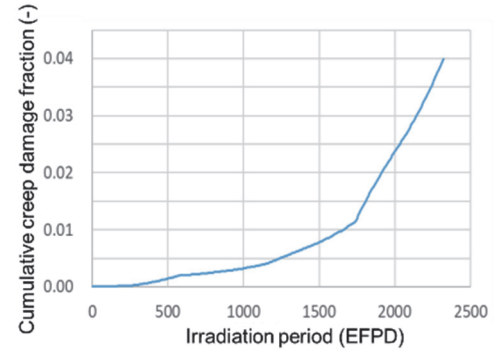

(a) Inner core fuel

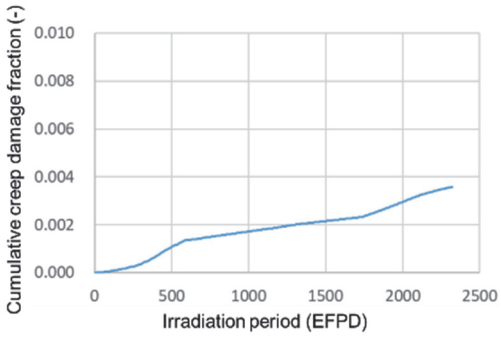

(b) Outer core fuel

Fig. 4 Cumulative creep damage fraction history for peak power pin

which is well below the CDF target of 0.5 for normal operation, so there is sufficient margin for fuel integrity even with a conservative evaluation. **Figure 5** shows the analysis results for UTOP situation when the power is continuously increased without limit. Cladding failure occurs at power ratio above 2.2 in UTOP. This result was used as the fuel failure criterion in the UTOP transient analysis.

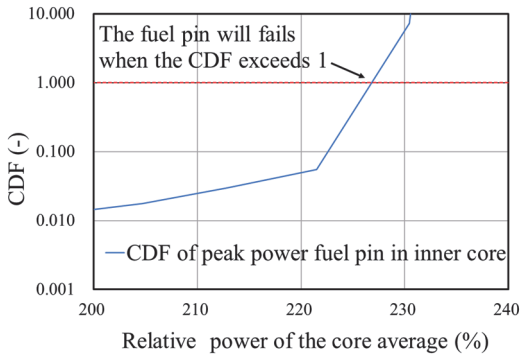

Fig. 5 Power transition vs CDF in UTOP Situation

3. ULOF Transient Analysis

Figure 6 shows the results of the ULOF analysis. As shown in Fig 6(a), the flow rate decreased rapidly after the start of the ULOF due to a pump failure. At this time, because the electromagnetic pump has no rotational inertia, the flow rate was halved about 2 seconds after the start of the event. On the other hand, the power also decreased because a large negative reactivity was inserted by GEM in response to the

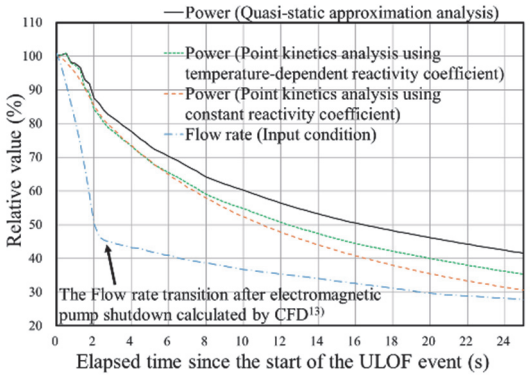

(a) Power and core flow rate transition

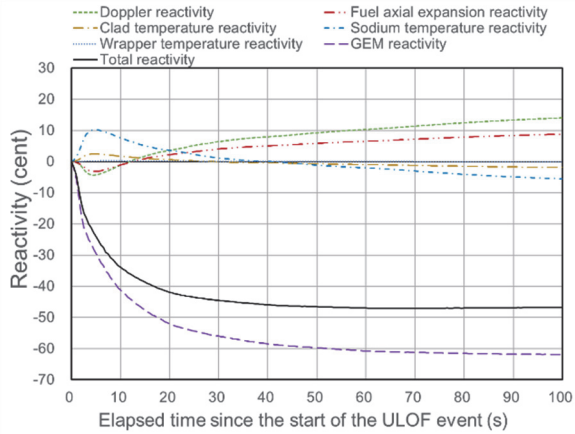

(b) Transition of reactivity by point kinetics analysis with constant reactivity coefficient

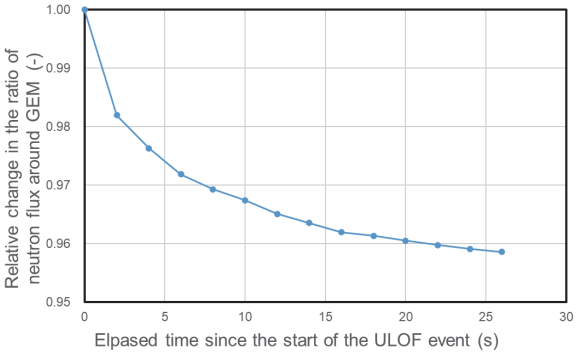

(c) Transition of the relative neutron flux of assembly adjacent to the GEM compared to the average change in the core by improved quasi-static approximation.

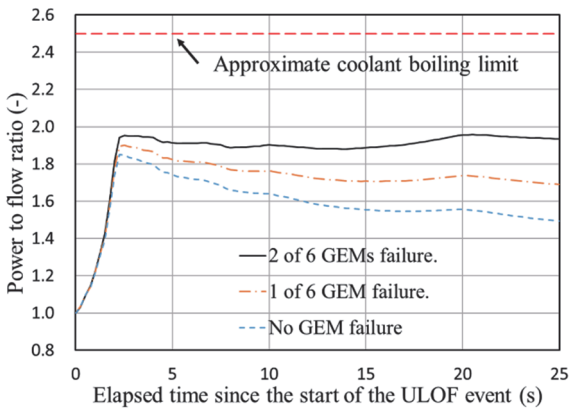

(d) P/F transition by improved quasi-static approximation

Fig. 6 ULOF analysis results

decrease in flow rate as shown in Fig. 6(b). After that, as the fuel temperature began to drop, positive doppler reactivity was inserted, but the effect was limited by the small power defects in the metal fuel core due not only to small absolute value of doppler coefficient but also to small fuel temperature drop.

The power after 6 seconds from the start of the event is affected by whether the reactivity coefficient is constant or temperature dependent on point kinetics analysis. This result indicates that point kinetics analysis with constant reactivity coefficients may give non-conservative results. Furthermore, the results of the improved quasi-static approximation analysis evaluated the power ratio higher than that of the point kinetics analysis. The reason is that, as shown in Fig. 6(c), the neutron flux of assembly adjacent to the GEM decreases with time by about 4% compared to the core average, an effect due to the spatial change of the neutron flux that cannot be accounted for by point kinetics. This neutron flux decrease results in a smaller negative GEM reactivity, leading to higher power compared to the evaluation using point kinetics evaluation.

As shown in Fig. 6(d), even when considering the failure of two GEMs, the power to flow ratio (P/F) remains below 2.0 in the analysis with quasi-static approximation, indicating that it is possible to avoid coolant boiling without SASS.

4. UTOP Transient Analysis

Figure 7 shows UTOP analysis results. As with the ULOF transient analysis, Fig. 7(a) shows that the evaluation of the point kinetics using a constant reactivity coefficient was not conservative. Furthermore, the results of the point kinetics and the quasi-static approximation were in close agreement up to 15 s after the start of the UTOP event, but the power rate of the point kinetics was estimated to be smaller thereafter. As shown in Fig. 7(b), the neutron flux distribution was distorted by the control rod withdrawal. However, the point kinetics analysis evaluates that the neutron flux throughout the core increases with the initial distribution, resulting in the underestimation of the power transition due to increased negative reactivity feedback such as the Doppler effect in the core center where the reactivity worth is large.

Based on the fuel transient behavior evaluation, when the core average power ratio exceeded approximately 2.2, the CDF exceeded 1 and pin failure occurred. Therefore, the fuel pin failure occurred approximately 42 seconds after the start of the ULOF event. According to the point kinetics analysis, the activation time of the SASS was 30 seconds after the start of the event, considering the coolant transport delay and the temperature time constant of the SASS temperature sensing alloy. This evaluation does not take into account the increase in coolant temperature around the BCR equipped with SASS due to the power distortion by the withdrawal of the PCR. Furthermore, the average core power is underestimated by approximately 5% at 30 seconds. Therefore, the activation time of the SASS in the point kinetics was estimated to be later due to these factors. There is a 12 second margin between the time of the SASS activation and the time of cladding failure, and the BCR requires about 3 seconds to be fully inserted after SASS activation[16], which is sufficient time for the SASS to shut down the reactor. Therefore, the SASS provides sufficient margin to prevent pin failure under the conservative estimate.

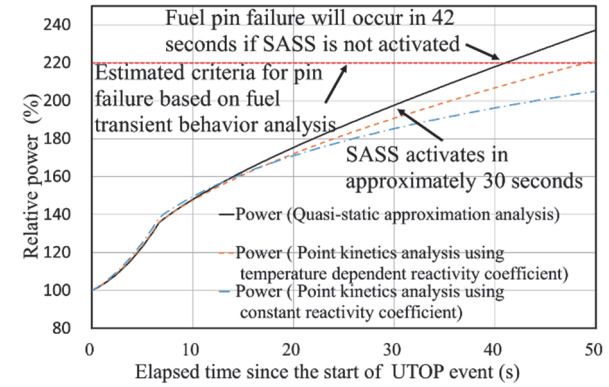

(a) Power transition

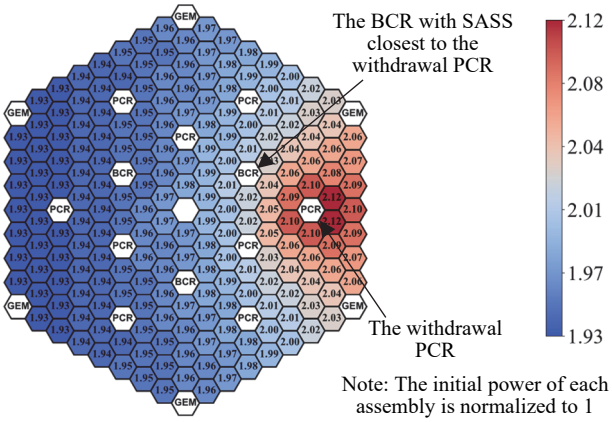

(b) Power increasing rate distribution at 30 seconds

Fig. 7 UTOP analysis results

5. ULOHS Transient Analysis

Figure 8 shows ULOHS analysis results. As shown in Fig. 8(a), the power rate was maintained at 100% for about 50 seconds after the start of the event. This is because the core temperature does not change until the hot pool coolant reaches the core inlet. After that, as the inlet temperature rises, the grid plate supporting the core expands, and the gap between the fuel assemblies widens, inserting continuous negative reactivity as shown in Fig. 8(b). The core power also decreased to the decay heat level in about 600 seconds. The coolant temperature also peaked at about 650°C and began to decrease. This is because the cooling by RVACS due to the rise in the reactor vessel temperature was balanced with the decay heat. The other reactivities besides grid plate expansion are balanced between positive and negative factors, and the grid plate expansion reactivity is dominant in ULOHS. Since the grid plate expansion reactivity is dependent on the inlet temperature, it is possible to provide continuous negative reactivity even when considering positive reactivity feedback during power reduction, allowing the system to transition to a hot standby state without relying on shutdown system.

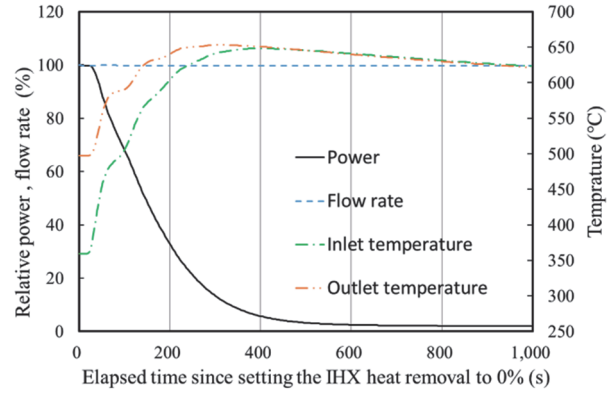

(a) Transition of power and coolant temperature

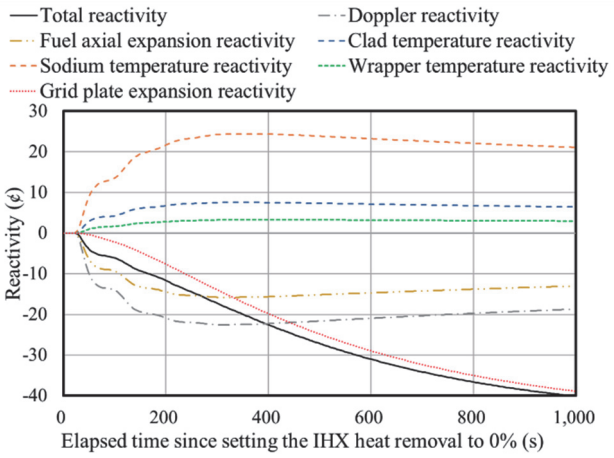

(b) Transition of reactivity

Fig. 8 ULOHS analysis results

V. Conclusion

The safety enhanced core satisfied the design criteria for nuclear core characteristics and fuel behavior. Furthermore, the core could prevent pin failure and coolant boiling during all ATWS events without radial expansion reactivity by safety measures such as GEM, SASS, and RVACS. This study showed that the point kinetics analysis method might underestimate the GEM reactivity. Therefore, when evaluating ULOF events using point kinetics for a core with GEM, it is necessary to correct for this effect. In addition, we confirmed that point kinetics underestimates power because of power distortion by control rod withdrawal. Furthermore, the ULOHS analysis revealed that subcriticality and stable cooling are maintained by inherent reactivity feedback and RVACS, respectively.

Acknowledgment

This research used resources of “Program to Support the Development of Innovative Nuclear Power Technologies in Response to Society's Needs” of the Ministry of Economy, Trade and Industry.

References

1) Y. I. Chang, et al. “Advanced burner test reactor preconceptual design report,” No. ANL-ABR-1. Argonne National Lab. (ANL), Argonne, IL (United States), (2008).
2) B. S. Triplett, E. P. Loewen, and B. J. Dooies. “PRISM: a competitive small modular sodium-cooled reactor,” *Nuclear Technology* **178**[2], 186-200 (2012).
3) A. E. Dubberley, et al. “SUPERPRISM OXIDE AND METAL FUEL CORE DESIGNS,” *Proceeding of the International Conference on Nuclear Engineering (ICONE) 8*, 2-6 (2000).
4) S. Nakanishi, T. Hosoya, S. Kubo, S. Kotake, M. Takamatsu, T. Aoyama, I. Ikarimoto, J. Kato, Y. Shimakawa, K. Harada. “Development of passive shutdown system for SFR,” *Nuclear Technology*, **170**[1], 181-188 (2010).
5) M. M. Uematsu, et al. “Fuel and core design studies on metal fuel sodium-cooled fast reactor (4), (5) and (6)." Joint research report for JFY2009 – 2012 (2012),” Japan Atomic Energy Agency, JAEA-Research 2012-041, (2013) [in Japanese].
6) K. Nakamura, et al. "Reactions of uranium-plutonium alloys with iron." *Journal of Nuclear Science and Technology*, **38**[2], 112-119 (2001).
7) INTERNATIONAL ATOMIC ENERGY AGENCY. “Absorber Materials, Control Rods and Designs of Shutdown Systems for Advanced Liquid Metal Fast Reactors,” *IAEA-TECDOC-884*, IAEA, Vienna, 118-119 (1996).
8) K. Yokoyama, T. Hazama, K. Numata, T. Jin. “Development of comprehensive and versatile framework for reactor analysis, MARBLE, ” *Annals of Nuclear Energy*, **66**, 51-60 (2014).
9) K. Sugino et al. “Fast reactor nuclear data set UFLIB.J40 and JFS-3-J4.0 based on JENDL-4.0,” Japan Atomic Energy Agency, JAEA-Data/Code 2011-017, (2011).
10) K. Sugino, K. Takino. “Development of neutron transport calculation codes for 3-D hexagonal geometry (2). Improvement and enhancement of the MINISTRI code,” Japan Atomic Energy Agency, JAEA-DATA/CODE-2019-011, (2020).
11) T. Ogata, et al. “Development and Validation of ALFUS: An Irradiation Behavior Analysis Code for Metallic Fast Reactor Fuels,” *Nuclear Technology*, **128**, 113 (1999).
12) T. Hashimoto, R. Kawabe. “Development of a dynamic analysis program for LMFBR plants,” *Trans. Am. Nucl. Soc.*;(United States) 45.CONF-831047- (1983).
13) G. Grandjean, et al. “Development of an innovative small sodium-cooled fast reactor (12) 3D thermal hydraulic transient analysis of RVACS heat removal characteristics”, Atomic Energy Society of Japan, 2022 Fall Meeting, 3F08, 2022.
14) S. Takeda, T. Takeda, S. Fuchita, T. Kitada. “Development of an Improved Quasi-Static Transient Analysis Code Based on Three-Dimensional Sn Nodal Transport Theory for Fast Reactor,” *Annals of Nuclear Energy*, **143**, (2020).
15) S. Fuchita, et al. “Core Concept of Innovative Small SFR with Metal Fuel for Deployment in Japan”, *Proceeding of International Symposium on Zero-Carbon Energy Systems*, A12-1, 10 January 2023, Tokyo, Japan, (2024) [in press].
16) Y. Chikazawa, et al. “Conceptual design study of small sodium cooled reactors,” JNC TY9400 2005-004, 2005. [In Japanese]